Pergamon

Scripta Metallurgica et Materialia, Vol. 33, No. 3, pp. 427-432, 1995

0956-716X/95 $9.50 + .00

0956-716X(95)00261-8

OBSERVATIONS OF PRECIPITATION IN A PARTICLE-REINFORCED Al-Cu-Mg ALLOY WITH 20% SILICON

P.M. Bronsveld[1], M.J. Starink[2], M. Verwerft[3], J.Th.M. de Hosson[1] and P. van Mourik[4]

[1] Department of Applied Physics, Materials Science Centre, University of Groningen, Nijenborgh 4, 9747 AG Groningen, The Netherlands
[2]Formerly with Laboratory of Materials Science, Delft University of Technology
Currently Department of Engineering Materials, University of Southampton, Highfield, Southampton S017 1BJ, United Kingdom
[3]Formerly with Department of Applied Physics, University of Groningen
Currently Centre for Nuclear Energy, Boeretang 200, B-2400 Mol, Belgium
[4]Laboratory of Materials Science, Delft University of Technology, Rotterdamseweg 137, 2628 AL Delft, The Netherlands

(Received January 5, 1995)
(Revised March 13, 1995)

1. Introduction

The wear resistance of aluminium alloys can be improved by the introduction of finely dispersed hard particles (1), e.g. a fine dispersion of silicon particles can be obtained by rapid solidification of a molten aluminium alloy with a high silicon content (2). Metals reinforced by dispersed (ceramic) particles (Metal Matrix Composites or MMCs) are produced via various routes, e.g. mixing liquid metal with ceramic particles (compocasting) or by mixing solid metal powder with ceramic particles. This powder metallurgy route generally avoids the formation of detrimental reaction layers at the particle/matrix interface. The ageing of a powder-metallurgical Al-20at%Si-1.5at%Cu-1.1at%Mg (ASCM) alloy reinforced with 10 vol% aluminiumoxide (Al_2O_3) particles was recently studied (3,4,5). This alloy combines two reinforcing components (silicon and Al_2O_3 particles) with age hardening of the Al-rich phase. The presence of dispersed particles in solid-quenched (SQ) aluminium alloys generally influences the kinetics and sequences of precipitation, as compared to corresponding unreinforced alloys (6). However, the Al_2O_3 particles in this alloy have very little influence on precipitation (3,4,5): during ageing at 453 K, for instance, the maximum hardness is reached after 4 hours for both reinforced and unreinforced alloys (5). This maximum hardness can be related with Q-phase ($Al_5Cu_2Mg_8Si_6$) precipitation (4,5). A needle-shaped semi-coherent precursor Q phase precipitating in SQ 2014 Al-alloy as well as in SQ 2014 Al-MMC was recently reported (7). For compositions corresponding to 2014 Al, it can be assumed that precipitation in the SQ alloy starts from a supersaturated monophase (7). For the ASCM alloys it was shown, that also after solid quenching large amounts of Q phase were present (4,5).

The equilibrium hexagonal Q phase is incoherent with the cubic Al-rich matrix. Hence it is unlikely that hexagonal Q-phase precipitates are directly responsible for the hardness increase, observed on ageing the SQ ASCM alloys. Therefore it was decided to perform a TEM investigation of precipitation in the ASCM alloy with Al_2O_3 particles.

2. Experimental Procedures

2.1. Production Route

The investigated alloy was made available by Showa Denko, Japan. The base alloy was rapidly solidified by gas atomisation (cooling rate about 10^4 to 10^6 K/s, see Ref. 8), yielding fine powder (sizes range from 1 to 100 μm, with a median size of 25 μm, see Ref. 9). The powder was mixed with Al_2O_3 particles, in order to obtain a mixture with 10 vol % Al_2O_3 particles. This mixture was extruded at about 670 K, yielding round bars of about 20 mm diameter. This condition will be referred to as AE (as-extruded). In Table 1, the chemical composition of the alloy is presented. Main impurities (as measured by X-ray fluorescence) are: Ni (~0.02 at%), Zn (~0.01 at%), Ti(~0.006 at%) and Cr (~0.005 at%).

2.2. Heat Treatment

Specimens were cut from the extrudate and enclosed in quartz capsules. These enclosed specimens were solution treated for 10 min at 763 K. Subsequently the specimens were quenched in water at room temperature and stored at room temperature for about one day. These specimens will be indicated by SQ. Other specimens were aged at 453 K after quenching for 1 and 4 hours. Besides, for a confirmation experiment, encapsulated specimens were solution annealed (10 minutes at 763), water-quenched, aged for 1 h and for 4 h at 453 K, stored at 80 K before thinning by grinding and ion milling at liquid nitrogen temperature, and subsequently studied by TEM.

2.3. TEM

Transmission Electron Microscopy (TEM) samples were prepared by ion milling using a commercially available GATAN line of devices. A JEOL 200CX microscope was used together with EDAX/Philips.

2.4. X-Ray Diffraction

Experimental details of the diffraction experiments are given in Ref. 5.

TABLE 1
Composition of the ASCM10 Alloy

Al_2O	Si		Cu		Mg		Fe	
	alloy	base	alloy	base	alloy	base	alloy	base
vol % *)	wt%	at%	wt%	at%	wt%	at%	wt%	at%
10.4	16.9	19.6	2.97	1.52	0.77	1.03	0.20	0.11

*)Calculated from measured weight percentages using the densities of the ASCM base alloy, 2.67 g/cm^3 and of α-Al_2O_3 (corundum) 3.98 g/cm^3.

3. Results

3.1. As-Extruded

An optical micrograph of the AE ASCM10 alloy is presented in Fig. 1. No clustering of Al_2O_3 particles (black) or Si particles (grey) is observed. However some banding of the Al_2O_3 particles in the extrusion direction does occur. The sizes of the Al_2O_3 particles range from 1 to 6 μm (average about 2 μm), the sizes of the silicon particles range from 2 to 10 μm (average about 4 μm). X-ray diffraction shows that the AE alloy contains Si, θ (Al_2Cu), Q ($Al_5Cu_2Mg_8Si_6$), Al_7Cu_2Fe phase precipitates and α-Al_2O_3 particles (5). EDAX element analysis of the precipitates observed in the as-extruded alloy with TEM confirmed the presence of these precipitates. No other non-matrix phases were observed.

3.2. Solid-Quenched

X-ray diffraction has shown (3) that the SQ alloy contains Si, Q and Al_7Cu_2Fe phase precipitates. EDAX element analysis of the precipitates observed in the SQ alloy with TEM confirmed the presence of these precipitates. As expected (see 3-5) the θ-phase precipitates, which are soluble at the solution temperature (see Ref. 10), had dissolved during the solution treatment. This is valid for the majority of the areas studied. Only in one case a θ-phase particle was observed after solid quenching. This atypical observation is neglected. The insoluble Fe containing precipitates and the partially soluble Q-phase precipitates (see Refs. 11,12) were still present. In addition to these non-coherent precipitates, spherically shaped coherent precipitates were observed at very few areas of the matrix (see Fig. 2). The selected area diffraction pattern of these precipitates and surrounding matrix (Fig. 2) indicates that these precipitates are coherent with the matrix. With an average diameter of about 10 nm these precipitates are very small. The precipitate has as yet not been identified. (For further discussion, see Section 4). Due to the plastic relaxation of the stresses around misfitting Si and Al_2O_3 particles (see Ref. 5) misfit dislocations are present around these particles (see Fig. 3).

3.3. Solid-Quenched+Aged

After 1 hour of ageing at 453 K, disc-shaped precipitates have appeared over nearly the entire matrix (Fig. 4). These precipitates are parallel to the cubic planes of the Al-rich matrix, implying semi-coherency. The diameter of the precipitates is about 70 nm. Dislocation networks around the particles were observed. In the

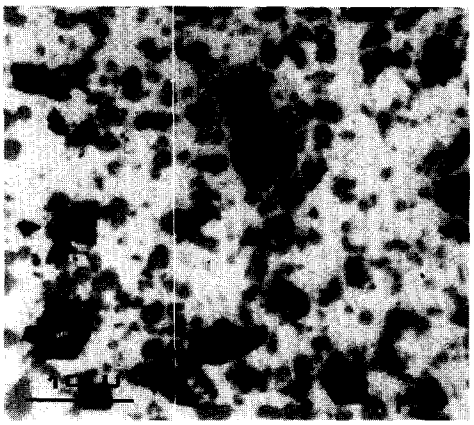

Figure 1. Optical micrograph of AE-ASCM10 with Si imaged grey and Al_2O_3 black.

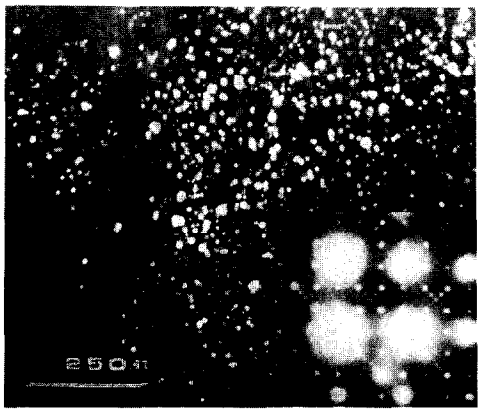

Figure 2. TEM micrograph of coherent precipitates in SQ-ASCM10 with its diffraction pattern.

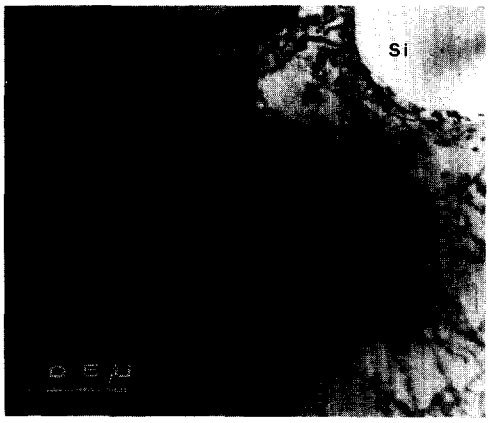

Figure 3. TEM micrograph of dislocation structures around Si particles in SQ-ASCM10.

Figure 4. TEM micrograph of precipitates in SQ and aged (1 hr at 453 K) ASCM10.

additional confirmation experiment, this observation was reproduced. Selected area diffraction and dark field imaging (Fig. 5) revealed, that the precipitates concerned were θ' (Al_2Cu). After 4 hours of ageing, incoherent precipitates were present, that were not disc-shaped. Analogous observations were obtained in the confirmation experiment. Selected area diffraction and dark field imaging of an area containing a number of these precipitates is shown in Fig. 6. The diffraction pattern appears like a powder pattern (no preferential orientation of the particles). The values for the interplanar spacings, d_{hkl}, obtained from this pattern are presented in Table 2. All the observed d_{hkl}-values can be attributed to d_{hkl}-values of the Q-phase from literature (see Table 2). Q and Al_7Cu_2Fe precipitates remained present during ageing. This was confirmed by selected area diffraction and dark field imaging. EDAX analysis confirmed the presence of the corresponding elements.

4. Discussion

Hardness measurements have shown that during room-temperature ageing directly after quenching the hardness increases within a few hours (3). DSC measurements (3) confirmed that this increase in hardness

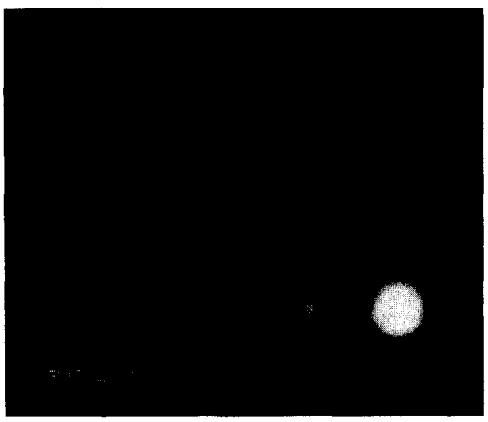

Figure 5. θ' precipitates in SQ and aged (1 hr at 453 K) ASCM10 with its diffraction pattern.

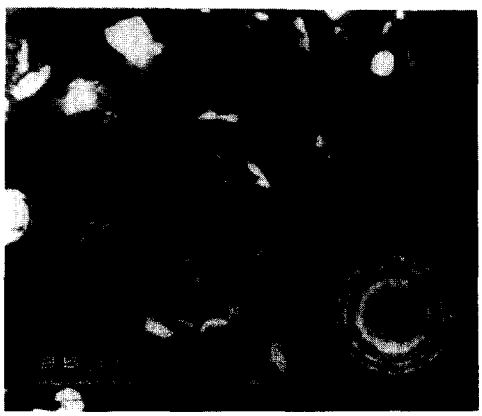

Figure 6. Q precipitates in SQ and aged (4 hrs at 453 K) ASCM10 with its diffraction pattern.

TABLE 2
Experimental d_{hkl}-Values (nm) Compared with Literature Values (nm) of d_{hkl} of Relevant Phases (Ref. 13)

experimental	literature Q $Al_5Cu_2Mg_8Si_6$		β′ Al_8Mg_5		S′ Al_2CuMg		θ′ Al_2Cu		Al_7Cu_2Fe	
	d_{hkl}	hkl	d_{hkl}	hkl	d_{hkl}	hkl	d_{hkl}	hkl	d_{hkl}	hkl
	0.9000	100								
	0.5197	110								
0.442	0.4500	200	0.4339	200	0.4530	020	—	—	0.4480	110
	0.4017	001								
	0.3669	101								
0.336	0.3402	210	0.3395	203	0.3345	012	0.3337	101	0.3324	113
0.325	0.3178	111	0.3216	211	0.3289	111	—	—	0.3206	104
	0.3000	300								
	0.2997	201								
0.254	0.2598	220	0.2505	220	0.2579	112	—	—	—	—
	0.2596	211								
	0.2496	310								
	0.2404	301								
0.222	0.2250	400	0.2205	313	0.2265	040	—	—	0.2215	221
	0.2182	221								
	0.2120	311								
0.206	0.2065	320	0.2074	314	0.2065	103	0.2046	112	0.2041	223
	0.2009	002								
	0.1963	410								
	0.1960	102								
	0.1874	112								
	0.1837	321								
	0.1834	202								
0.177	0.1765	411	0.1789	413	0.1765	202	0.1749	103	0.1764	314
	0.1732	330								
0.155	0.1565	312	0.1546	334	0.1548	203	—	—	0.1549	402
0.132	0.1312	332	0.1347	434	0.1313	311	0.1323	031	0.1324	424
0.120	0.1191	432	0.1198	444	0.1177	303	0.1183	204	0.1199	434
0.109	0.1091	442	—	—	0.1096	333	0.1112	303	0.1093	443
0.098	0.0980	204	—	—	0.0979	421	0.0975	411	—	—
0.079	0.0795	444	—	—	—	—	—	—	—	—

is related to an exothermic reaction (i.e. the formation of precipitates or GP-zones). As the first SQ specimens were stored at room temperature for about one day before TEM investigation, the fine coherent precipitates observed in these SQ samples (see Fig. 2) are probably related to this reaction.

During 4 hours of ageing at 453 K the hardness of the ASCM alloy increases to its maximum. Within the first hour of ageing about 90 % of this hardness increase is achieved, while the lattice parameter of the Al-rich phase starts to increase (see Ref. 5). At these stages of ageing, possibly present GP zones are assumed to dissolve completely (cf. Refs. 5 and 7). In the present investigation, the only semi-coherent precipitates observed after 1 h of ageing at 453 K, were the θ' precipitates (see Section 3.3). From Refs. 4 and 7 follows that the precipitation effect of the $Al_5Cu_2Mg_8Si_6$-phases (Q or Q') preceeds the precipitation effect of the Al_2Cu-phases (θ/θ'), although both effects show overlap. The needle-shaped Q' phase is held responsible for most of the hardening in the AA 2014 alloy (see Ref.7). For the present alloy, no indications for the occurrence

of Q'-phase were found after 1 h ageing at 453 K, nor in the first SQ specimens nor in the confirmation experiment. It can be shown that $Al_5Cu_2Mg_8Si_6$-precipitation has very little effect on the Al-rich phase lattice parameter (contributions from Cu, Mg and Si precipitation balance, see Ref. 5). Apparently, at this stage of ageing, semi-coherent θ' phase precipitates along with the equilibrium Q phase. Correspondingly, diffraction lines of equilibrium θ phase appeared after 4 h of ageing at 453 K (Ref. 5). The appearance of this phase implies a hardness decrease (cf.Ref. 5).

The origin of the apparent absence of Q' phase in ASCM10 compared with the AA2014 alloy can be twofold. Firstly, small compositional differences might be taken into account. However, the increased Cu/Mg ratio of the AA2014 would even enhance θ' formation. The important difference between the AA2014 (monolithic and composite) and the ASCM10 alloy is of course the increased volume content of misfitting particles in the latter alloy: about 20 vol% of silicon particles and about 10 vol% of Al_2O_3 particles. On the basis of the reasoning in Ref. 5, the density of misfit dislocations in the ASCM10 alloy is estimated at least twice as large as in the AA2014 MMC. The presence of reinforcing particles in the AA2014 MMC was found to enhance θ' precipitation, but to decelerate Q' precipitation (Ref.7). Hence, the absence of Q' phase in the ASCM alloy is probably due to the increased dislocation density, favouring θ' precipitation. The foregoing indicates strongly, that the hardness changes observed for the ASCM10 alloy are largely due to the θ'/θ-phase precipitation/coarsening.

5. Conclusion

By a TEM study it was confirmed that the as-extruded ASCM10 alloy contains Si, θ (Al_2Cu), Q, Al_7Cu_2Fe-phase precipitates and α-Al_2O_3 particles. During solution treatment all θ-phase precipitates dissolve, whereas the Q-phase precipitates dissolve only partly. During subsequent ageing at 453 K, precipitation of θ' occurs concomitantly with $Al_5Cu_2Mg_8Si_6$-precipitation, the latter precipitation only involves the equilibrium modification of Q phase.

Acknowledgement

The authors are indebted to Dr. Inz. J. Duszczyk (Laboratory of Materials Science, Delft University of Technology) for providing the alloy.

References

1. D. Bialo, J. Duszczyk, A.W.J. de Gee, G.J.J. van Heijningen and B.M. Korevaar, Wear 141, 291 (1991).
2. J.L. Estrada and J. Duszczyk, J. of Mater. Sci. 25, 886 (1990).
3. M.J. Starink, V. Jooris and P. van Mourik, Proc. of the 1st ASM Heat Treatment and Surface Engineering Conference, Amsterdam, The Netherlands, 22-24 May 1991, p.85, E.J. Mittemeijer ed., Trans Tech Publications Ltd, Zürich, Switserland, 1992.
4. M.J. Starink, V. Jooris and P. van Mourik, Proc. of the 12th RISØ International Symposium on Metal Matrix Composites-Processing, Microstructure and Properties, 2-6 September 1991, p.675, Roskilde, Denmark, N. Hansen et al., eds.
5. M.J. Starink, V. Abeels and P. van Mourik, Mater. Sci. Eng.A163, 115 (1993).
6. J. M. Papazian, Metall. Trans. 19A, 2945 (1988).
7. I. Dutta, C.P.Harper and G.Dutta, Metall. and Mater. Trans. 25A, 1591 (1994).
8. L. Estrada and J. Duszczyk, J. of Mater. Sci.25, 886 (1990).
9. J.H. ter Haar and J. Duszczyk, Mater. Sci. and Eng.A135, 65 (1991).
10. L.F. Mondolfo: Aluminium Alloys: Structure and Properties, p. 253, Butterworths, London (1976).
11. A.K. Gupta, M.C. Chaturvedi and A.K. Jena, Mater. Sci. and Techn. 5, 52 (1989).
12. A.K. Gupta, M.C. Chaturvedi and A.K. Jena, Metall. Trans. 24A, 2181 (1993).
13. P. Villars and L.D. Calvert, Pearson's Handbook of Crystallographic Data for Intermetallic Phases, vols. 1 & 2, American Society for Metals, Ohio (1985).